1

1 Disentangling tropicalization and deborealization in marine

2 ecosystems under climate change

3

- 4 Matthew McLean^{1,12*}, David Mouillot², Aurore A. Maureaud^{3,4}, Tarek Hattab⁵, M. Aaron
- 5 MacNeil^{1,6}, Eric Goberville⁷, Martin Lindegren⁴, Georg Engelhard^{8,9}, Malin Pinsky¹⁰, Arnaud
- 6 Auber¹¹

7

- 8 Department of Biology, Dalhousie University, Halifax, Nova Scotia, Canada, B3H 4R2.
- 9 ²MARBEC, Univ Montpellier, CNRS, IFREMER, IRD, 34095 Montpellier Cedex, France.
- ³Center for Biodiversity and Global Change, Department of Ecology & Evolutionary Biology,
- 11 Yale University, New Haven, CT 06520, USA.
- ⁴Centre for Ocean Life, c/o National Institute of Aquatic Resources, Technical University of
- Denmark, Kemitorvet Bygning 202, 2800 Kgs. Lyngby, Denmark.
- ⁵MARBEC, Univ Montpellier, CNRS, Ifremer, IRD, Avenue Jean Monnet, 34200 Sète, France.
- ⁶Ocean Frontier Institute, Dalhousie University, Halifax, Nova Scotia, Canada, B3H 4R2.
- ⁷Unité Biologie des Organismes et Ecosystèmes Aquatiques (BOREA), Muséum National
- 17 d'Histoire Naturelle, Sorbonne Université, Université de Caen Normandie, Université des
- 18 Antilles, CNRS, IRD, 75231 Paris Cedex 05, France.
- 19 ⁸Centre for Environment, Fisheries & Aquaculture Science (Cefas), Pakefield Road, Lowestoft
- 20 NR33 0HT, UK.
- 21 ⁹Collaborative Centre for Sustainable Use of the Seas (CCSUS), University of East Anglia,
- Norwich NR4 7TJ, UK.
- 23 ¹⁰Department of Ecology, Evolution, and Natural Resources, School of Environmental and
- 24 Biological Sciences, Rutgers, The State University of New Jersey, New Brunswick, NJ 08901.
- 25 ¹¹IFREMER, Laboratoire Ressources Halieutiques, 150 quai Gambetta, BP699, 62321
- 26 Boulogne-sur-Mer, France.
- 27 ¹²Lead Contact
- *Correspondence: mcleami@gmail.com

29

30 Key words: climate change, community temperature index, fisheries, marine ecology

31

32

33

34

Summary

As climate change accelerates, species are shifting poleward and subtropical and tropical
species are appearing in temperate environments 1-3. A popular approach for characterizing such
responses is the community temperature index (CTI), which tracks the mean thermal affinity of
a community. Studies in marine ⁴ , freshwater ⁵ , and terrestrial ⁶ ecosystems have documented
increasing CTI under global warming. However, most studies have only linked increasing CTI
to increases in warm-affinity species. Here, using long-term monitoring of marine fishes across
the Northern Hemisphere, we decomposed CTI changes into four underlying processes -
tropicalization (increasing warm-affinity), deborealization (decreasing cold-affinity),
borealization (increasing cold-affinity), and detropicalization (decreasing warm-affinity) - for
which we examined spatial variability and drivers. CTI closely tracked changes in sea surface
temperature, increasing in 72% of locations. However, 31% of these increases were primarily
attributable to decreases in cold-affinity species, i.e., deborealization. Thus, increases in warm-
affinity species were prevalent, but not ubiquitous. Tropicalization was stronger in areas that
were initially warmer, experienced greater warming, or were deeper, while deborealization was
stronger in areas that were closer to human population centers or that had higher community
thermal diversity. When CTI (and temperature) increased, species that decreased were more
likely to be living closer to their upper thermal limits or to be commercially fished.
Additionally, warm-affinity species that increased had smaller body sizes than those that
decreased. Our results show that CTI changes arise from a variety of underlying community
responses that are linked to environmental conditions, human impacts, community structure,
and species characteristics.

Results and Discussion

- Fish communities worldwide are responding to global warming through shifts in mean thermal affinity, which can be represented by the community temperature index (CTI)^{4,7–9}. An increase in CTI necessarily implies an increase in the relative abundance of warm-affinity species. However, a key question is whether this is primarily due to increases in the total abundance of warm-affinity species or to decreases in the total abundance of cold-affinity species. To resolve
- 'tropicalization' (increasing abundance of warm-affinity species)

this, we decomposed CTI changes into four underlying processes:

- 'deborealization' (decreasing abundance of cold-affinity species)
- 'borealization' (increasing abundance of cold-affinity species)
- 'detropicalization' (decreasing abundance of warm-affinity species)
 - Here, we define warm-affinity and cold-affinity species locally within each community: warm-affinity species are those whose thermal affinity is higher than the mean of the community and cold-affinity species are those whose thermal affinity is lower than the mean. Additionally, whereas past literature has used the term 'tropicalization' to describe increasing CTI⁷ or poleward distribution shifts^{3,10–12}, we explicitly use this term to refer to an increase in warm-affinity species. We applied this approach to fish communities using scientific monitoring data from 558 grid cells covering 12 marine regions across the Northern Hemisphere that showed contrasting changes in sea surface temperatures (SST) over the period 1990 to 2015. We calculated the relative strength of each underlying processes in each grid cell and identified which process was strongest when CTI increased or decreased. Finally, we examined the potential influences of environmental conditions, human impacts, and community structure on differences in the strength of the underlying processes and examined differences between species contributing to opposite processes (e.g., borealization vs. deborealization).

Mean-annual SST increased in 72.4% (404) of grid cells between 1990 and 2015 with a mean of $0.23 \pm 0.007^{\circ}$ C decade⁻¹ (mean \pm standard error), while it decreased in 27.6% of cells (154) with a mean of $-0.10 \pm 0.008^{\circ}$ C decade⁻¹ (Figure 2A). CTI closely mirrored SST (Pearson's correlation: 0.47), increasing in 71.3% (398) of cells, with a mean of $0.28 \pm 0.013^{\circ}$ C decade⁻¹ (Figure 2B), and decreasing in 28.7% (160), with a mean of $-0.14 \pm 0.014^{\circ}$ C decade⁻¹ (Figure 2B). Increases in CTI occurred primarily along the northeast coast of the United States, in the Scottish Seas, the North Sea, the Baltic Sea, the Barents Sea, and around the Aleutian Islands, while decreases were more prominent along the west and southeast coasts of the United States and in the Bering Sea (Figure 2B).

We next decomposed changes in CTI and quantified the strength of each underlying processes within each grid cell. Across all grid cells, tropicalization was the strongest process on average being dominant in 47% of cells, while detropicalization was the weakest, being dominant in only 7% of cells (Figure S1). Among the grid cells where CTI increased, tropicalization was stronger than deborealization in 68.6% (while deborealization was stronger in 31.4%) (Figure 2C). Hence, while past literature has focused extensively on increases in warm-affinity species and poleward distribution shifts^{3,7,11,13}, over one third of CTI increases were attributable to decreases in cold-affinity species. Among the grid cells where CTI decreased, borealization was stronger than detropicalization in 75% (Figure 2D). These patterns were clearly spatially structured, as tropicalization was stronger than deborealization along the east coast of the United States, in the Scottish Seas, the North Sea, the Baltic Sea, along the west coast of Norway, in the western Barents Sea, and around the Aleutian Islands. Deborealization was stronger in the Bering Sea, the Gulf of Mexico, and the eastern Barents Sea (Figure 2C). Borealization was stronger than detropicalization in nearly every region where CTI decreased, especially in the Bering Sea and along the west coast of the United States (Figure 2D).

To identify the biotic or abiotic conditions associated with each process, we next modelled the difference in the strength of (i) tropicalization vs. deborealization when CTI increased, and (ii) borealization vs. detropicalization when CTI decreased. Thus, the difference in the strength of the processes was the response variable (i.e., tropicalization minus deborealization; borealization minus deborealization). Explanatory variables were the rate of change in SST, initial (i.e., baseline) SST, mean-annual SST variation, depth, distance to the nearest human population center, mean maximum body size, community thermal diversity (CTDIV), and community thermal range (CTR) (see STAR methods and Table S2 for details). We used linear mixed effects models with Gaussian likelihood distributions where grid cells were the unit of observation and survey campaign was included as a random effect (i.e., varying intercept). When CTI increased, tropicalization was stronger than deborealization in cells that were initially warmer (effect size = 0.16 [0.07, 0.24; 95% CI]), experienced greater warming (effect size = 0.07 [0.02, 0.13]) or were deeper (effect size = 0.07 [0.02, 0.11]; Figure 3A). Deborealization was stronger than tropicalization in cells that were closer to human population centers (effect size = 0.07 [0.02, 0.11]) or that had greater community thermal diversity (effect size = -0.05 [-0.10,-0.01]; Figure 3A). When CTI decreased, borealization was stronger than detropicalization in cells that were initially warmer (effect size = 0.13 [0.01, 0.25]), had greater temperature increases (effect size = 0.07 [0.01, 0.12]) (or lower temperature decreases since CTI decreases are mostly associated with cooling), or were deeper (effect size = 0.06 [0.01, 0.11]; Figure 3B).

107

108

109

110

111

112

113

114

115

116

117

118

119

120

121

122

123

124

125

126

127

128

129

130

131

Theoretically, ignoring all factors other than temperature, when temperature and CTI are increasing, borealization and detropicalization should not occur, and when temperature and CTI are decreasing, tropicalization and deborealization should not occur. However, all four processes occurred to some extent in nearly every grid cell (Figure S1). We therefore hypothesized that there were mechanistic differences between species that explained this

anomaly. For instance, when CTI is increasing, species that contribute to borealization likely differ in some key features from species that contribute to deborealization. We identified differences between species contributing to (i) borealization vs. deborealization, and (ii) tropicalization vs. detropicalization, using linear mixed effects models with binomial likelihood distributions where species were the unit of observation and grid cell nested in survey campaign were included as random effects (see STAR methods and Table S3 for details). Thus, the binary response variable was whether a species was contributing to i) deborealization (0) or borealization (1), or to ii) detropicalization (0) or tropicalization (1). In grid cells where CTI increased, explanatory variables included maximum thermal limit, thermal range, maximum body size, and whether species are commercially fished. In grid cells where CTI decreased, the same explanatory variables were used except that minimum thermal limit was used in place of maximum thermal limit. When CTI increased, species contributing to borealization had higher maximum thermal limits (i.e., more tolerant of warming) (effect size = 0.72 [0.53, 0.91]) while species contributing to deborealization were more likely to be commercially fished (effect size = -0.34 [-0.49, -0.19]) and had wider thermal ranges (effect size = -0.16 [-0.28, -0.04]; Figure 4A). Similarly, species contributing to tropicalization had higher maximum thermal limits (effect size = 0.57 [0.38, 0.76]) and smaller body sizes (effect size = -0.17 [-0.24, -0.10]) and species contributing to detropicalization had wider thermal ranges (effect size = -0.15 [-0.27, -0.03]; Figure 4A). When CTI decreased, species contributing to borealization had wider thermal ranges than those contributing to deborealization (effect size = 0.17 [0.04, 0.29]). Species contributing to detropicalization had higher minimum thermal limits (effect size = -0.35 [-0.52, -0.17]), were more likely to be commercially fished (effect size = -0.26 [-0.44, -0.08]), and had smaller body sizes (effect size = 0.09 [0.01, 0.18]; Figure 4B) than those contributing to tropicalization.

132

133

134

135

136

137

138

139

140

141

142

143

144

145

146

147

148

149

150

151

152

153

154

155

Previous studies have documented large-scale changes in CTI but have not identified the underlying processes of these community thermal shifts^{3,4,6}. Unraveling these processes has clear implications for predicting future biodiversity responses under global warming, as well as potential impacts on community trait composition^{14,15} and their consequences for ecosystem structure and functioning^{16–18}. For example, communities increasing in CTI due to emigration or mortality of cold-affinity species (i.e., deborealization) could experience population crashes or local extinctions under future warming and could be considered conservation priorities^{19–21}. In contrast, communities increasing in CTI due to immigration or population growth of warmaffinity species (i.e., tropicalization) may have increased abundance and productivity despite changing composition^{8,22,23}, and could be resilient to well-managed fishing pressure.

While increases in CTI have been frequently linked to immigration or poleward distribution shifts by warm-affinity species^{3,10,13}, we observed that over one third of CTI increases were primarily explained by decreases in cold-affinity species (i.e., deborealization). This result has major implications for understanding climate change impacts on community structure, particularly as tropicalization and deborealization were spatially non-random and associated with environmental variation and human impacts. Tropicalization was stronger than deborealization in areas with warmer initial temperatures and areas with greater overall warming. This is consistent with previous studies showing that community thermal shifts depend not only on the rate of warming, but also baseline climate. For instance, Antão et al.²⁴ showed that in marine communities exposed to warming, species gains outpaced species losses under warmer initial conditions, and Lenoir et al.²⁵ showed that marine species track isotherms more rapidly in initially warm waters. These results are consistent with faster colonization and range edge expansion and slower extirpation and range edge contraction^{11,26}. These results may also be explained by more rapid dispersal and population growth in warmer environments. In marine organisms, the speed of metabolic and demographic processes increases with

temperature²⁷, and both range expansion by new species and population growth of existing species should occur more rapidly under warmer conditions. Warm species gains may also dominate in warmer environments due to the latitudinal gradient in species richness, as greater numbers and proportions of warm-affinity species are expected in warm, species-rich areas²⁸.

Tropicalization was generally stronger than deborealization in deeper areas, likely owing to greater vertical temperature refuge for cold-affinity species⁹. For instance, tropicalization was particularly strong along the east coast of the United States, in the Scottish Seas, and in the western Barents Sea. These regions are situated along deep, open shelves, which could enable cold-affinity species to temporarily seek refuge in cooler, deeper waters during warming episodes, preventing their loss locally²⁹. This is consistent with previous studies showing that relatively small shifts in depth may allow species to remain within their thermal niches^{9,30} In the North Sea, a system primarily characterized by tropicalization, many species have shifted to cooler, deeper waters over the last few decades³⁰. However, the North Sea is a relatively shallow, semi-enclosed ecosystem and Rutterford et al.³¹ showed that North Sea fishes will eventually be constrained by depth limitations, compressing habitat suitability and potentially driving local extinction. Thus, the increase or immigration of warm-affinity species could be currently out-pacing the decline or emigration of cold-affinity species, but this trend could reverse in the future if cold-affinity species are unable to find thermal refuge.

Areas characterized by deborealization or detropicalization, i.e., decreasing abundance, had greater community thermal diversity than areas characterized by tropicalization or borealization. One hypothesis could be that communities with higher thermal diversity have fewer vacant niches (i.e., niche saturation) and therefore fewer opportunities for immigration and establishment by new species^{32,33}. Communities with greater thermal diversity may also contain more species living closer to their thermal limits, and thus have greater potential for species losses or population declines due to temperature rises⁹. For instance, Burrows et al.⁹

showed that communities with greater thermal diversity may have higher sensitivity to temperature changes, as species near their thermal limits can be rapidly lost or gained²⁸.

Tropicalization and borealization were more common than deborealization or detropicalization. This suggests that habitat suitability is expanding for warm-affinity species faster than it is retracting for cold-affinity species²⁶. Hence, many cold-affinity species may be tolerant of current warming, yet future warming could trigger major losses, potentially shifting the balance between tropicalization and deborealization. Even when CTI decreased, detropicalization was rarely dominant, as warm-affinity species rarely showed strong decreases. While some areas did experience cooling during the study period, the average rate of cooling was roughly half of the rate of warming, and all regions have experienced long-term temperature rises. Thus, warm-affinity species appear to be less impacted by periods of mild cooling, and detropicalization should become increasingly rare under future warming.

Interestingly, we found that when CTI increased, some cold-affinity species increased and some warm-affinity species decreased, counter to expectation. This was primarily explained by thermal limits and apparent fishing pressure. Cold-affinity species that increased had higher maximum thermal limits than those that decreased, and those that decreased were more likely to be commercially fished. Because species were compared within the same grid cells, species with lower thermal maxima were living closer to their upper limits. Species decreases can therefore be attributed to temperature rises surpassing thermal tolerances as well as potential overfishing. Hence, both thermal tolerance and fishing pressure are shaping long-term changes in marine fish communities, and future community responses will be driven by the cumulative impacts of climate change and human pressure^{5,25,34}. The potential impacts of fishing were also highlighted by the finding that deborealization (i.e., decreasing abundance) was stronger in areas closer to human population centers.

When CTI increased, warm-affinity species that increased had smaller body sizes than those that decreased. Smaller-bodied species generally have faster growth rates, shorter generation times, and less parental investment, enabling populations to rapidly track environmental changes^{14,35,36}. Thus, small-bodied species whose upper thermal limits were not surpassed by temperature rises could rapidly increase in abundance following warming, particularly as warming elevates metabolic and demographic rates. In contrast, large-bodied species have slower growth rates and reproduce later in life, leading to slower population turnover and environmental tracking^{35,36}. Large-bodied species are also more susceptible to human impacts³⁷. Hence, even large-bodied species that are favored by temperature rises might be decreasing in abundance faster than they can reproduce, leading to population declines despite warm-water affinities.

While limited to fish communities from 12 marine regions over a 26-year period, our approach is applicable to other ecosystems and taxa and may help unravel the underlying processes of community thermal shifts at a global scale³⁸. Identifying how changes in species' distributions and abundances are impacting overall diversity and community dynamics will be key for planning future conservation and management efforts^{39–42}. Areas with net losses of coldaffinity species may require careful fisheries regulation, whereas areas gaining warm-affinity species may have increased productivity and exploitation opportunities^{8,23,43,44}. Overall, we found that over one third of CTI increases were more strongly explained by decreases in coldaffinity species than by increases in warm-affinity species, with significant roles of environmental conditions, human impacts, and community structure. Additionally, we found that species tendencies to increase or decrease in response to temperature changes were dictated by thermal limits and commercial fishing status. Future studies should link spatial patterns in the underlying processes of CTI to changes in seasonality, ocean currents, and other abiotic factors likely to be modified by climate change, as well as changes in fishing pressure and

human impacts. While past studies have documented extensive shifts in CTI, ours is the first to decompose CTI into underlying processes at a multi-continental scale, which could help in anticipating future changes in biodiversity under climate change and implementing adapted management strategies.

Acknowledgements

We acknowledge the MAESTRO group funded by the synthesis center CESAB of the French Foundation for Research on Biodiversity (FRB) and Filière France Pêche (FFP). M.M. and A.A. were supported by Electricité de France (RESTICLIM and ECLIPSE project), IFREMER (ECLIPSE project), Région Hauts-de-France and the Foundation for Research on Biodiversity (ECLIPSE project, contract no. astre 2014-10824). M.M. and M.A.M. were supported by the Natural Sciences and Engineering Research Council (Grant No. RGPBB/525590). M.A.M. was also supported by the Canada Research Chairs Program and the Ocean Frontier Institute. M.L. and A.A.M. were supported by VKR Centre for Ocean Life and a VILLUM research grant (No. 13159). M.L. was also supported by the European Union's Horizon 2020 research and innovation programme under Grant Agreement No 862428 (MISSION ATLANTIC) and No. 869300 (FutureMARES). M.L.P was supported by U.S. National Science Foundation #DEB-1616821.

Author contributions

A.A., D.M. and M.M. designed the research, A.A.M., T.H., and M.M. collected and processed the data, M.M. analyzed the data, and all authors contributed to conceptual development and writing.

278

279

Declaration of interests

280 The authors declare no competing interests.

281

282

Figure legends

- 283 Figure 1. The four underlying processes contributing to changes in CTI. Increases in CTI
- occur when the combination of tropicalization (red) and deborealization (orange) is stronger
- than the combination of borealization (blue) and detropicalization (purple). CTI increases can
- therefore be attributed to either topicalization or deborealization, whichever process is stronger,
- and CTI decreases can be attributed to either borealization or detropicalization, whichever
- 288 process is stronger.
- Figure 2. Maps showing the rate of change in SST and CTI along with differences in the
- strength of the underlying processes. Rate of change in SST (A) and CTI (B) across the 558
- 291 spatial sampling grid cells for the period 1990 2015. Differences in the strength of
- tropicalization and deborealization in grid cells where CTI increased (C), and differences in the
- strength of borealization and detropicalization in grid cells where CTI decreased (D). See also
- Figure S1, which shows average relative strength of each underlying process, Figure S2, which
- shows the area covered by each monitoring survey, Table S1, which provides details on the
- 296 monitoring surveys, Figure S3, which shows the method for calculating the strength of each
- 297 underlying process, and Figure S4, which compares the rate of change in CTI vs. (topicalization
- + deborealization) (borealization + detropicalization).
- 299 Figure 3. Results of linear mixed effects models of differences in the strength of
- 300 tropicalization and deborealization in grid cells where CTI increased (A), and of
- differences in the strength of borealization and detropicalization in grid cells where CTI
- decreased (B). Grey circles represent standardized effect sizes and black horizontal bars
- 303 represent 95% confidence intervals. In panel A, positive effects are associated with stronger
- tropicalization, and negative effects are associated with stronger deborealization. In panel B,
- 305 positive effects area associated with stronger borealization, and negative effects are associated
- with stronger detropicalization. See also Table S2, which shows the output summary for each
- 307 model.
- Figure 4. Results of linear mixed effects models of i) the probability that a species
- 309 contributed to borealization or deborealization, and ii) the probability that species
- 310 contributed to topicalization or detropicalization when CTI increased (A) and when CTI
- 311 decreased (B). Grey circles represent standardized effect sizes and black horizontal bars
- 312 represent 95% confidence intervals. Positive effects are associated with species that contributed
- 313 to borealization or tropicalization, and negative effects are associated with species that
- 314 contributed to deborealization or detropicalization. See also Table S3, which shows the output

315 316	summary for each model, and Table S4, which compares model results using different subsets of species based on quantiles of abundance changes.
317	
318	STAR METHODS
319	
320	RESOURCE AVAILABILITY
321	Lead Contact
322	Further information and requests should be directed to and will be fulfilled by the lead contact,
323	Matthew McLean (mcleamj@gmail.com).
324	
325	Materials Availability
326	This study did not generate new unique reagents.
327	
328	Data and Code Availability
329	This paper analyzes existing, publicly available data. Links for the datasets are provided in the
330	key resources table. This paper does not report original code. Any additional information
331	required to reanalyze the data reported in this paper is available from the lead contact upon
332	request.
333	
334	EXPERIMENTAL MODEL AND SUBJECT DETAILS
335	All fish monitoring data used in this study are freely available and open access; references and
336	links are provided in the Key resources table and Supplemental information. No experimental

models (animals, human subjects, plants, microbe strains, cell lines, primary cell cultures) were used in the study.

339

340

341

342

343

344

345

346

347

348

349

350

351

352

353

354

355

356

357

358

359

360

337

338

METHOD DETAILS

Fish community data

Thirteen bottom-trawl surveys from 12 marine regions across the northern hemisphere were used to examine changes in the community temperature index (CTI) in fish communities over a large geographic scale with substantial longitudinal, latitudinal, and depth gradients. All surveys used similar sampling protocols, where bottom trawls were towed for an average of 30 minutes and the species composition and abundances of all captured fishes were identified and recorded (see Table S1). Spatial coverage and resolution differed across surveys, and we therefore aggregated trawl surveys to 1° longitude × 1° latitude spatial grid cells. A 1° longitude × 1° latitude resolution was chosen to adequately capture both inter and intra-survey variation, to reveal gradients in community responses, to maximize data availability, and to match with the spatial resolution of the HadISST database (see 'Sea surface temperature' below). The length of time series also differed between surveys, and we therefore examined the period 1990 -2015, which maximized temporal overlap between surveys. Following Burrows et al.⁹, along the US West Coast, two surveys with overlapping spatial coverage but adjacent temporal periods were combined (see Figure S1 and Table S1). The combined data were inspected for discontinuities, and we verified that our main results and conclusions were robust to removing these data from the analyses. Because some surveys are conducted in multiple seasons, for each grid cell, we only used data for the quarter with the greatest number of years surveyed. Lastly, because of spatial and temporal heterogeneity in sampling effort both between and within grid cells, we performed a bootstrap sampling procedure. We randomly selected four trawl surveys

per grid cell, per year (four was the median number of trawls per cell, per year), recorded the resulting species' abundances, repeated this procedure 99 times, and calculated species' mean abundances across the 99 permutations. Only grid cells with with maximum sampling gaps of five years or less were considered (some surveys are only conducted every 3-5 years), resulting in a total of 558 cells. All survey abundance data were then $\log_{10}(x+1)$ transformed before analyses. While we recognize that aggregating bottom trawl data to a 1° longitude × 1° latitude scale creates species assemblages that are not true locally interacting biological communities, we use the term 'community' for consistency with existing literature on concepts such as the community temperature index and community thermal diversity.

Sea surface temperature (SST)

For each grid cell, we extracted mean-annual sea surface temperature (SST) and annual SST variation. Minimum and maximum SST were also initially considered, but later dropped because they were highly correlated with mean SST, but much less informative (i.e., never had discernable effects in statistical models). SST data for each grid cell were derived from the Hadley Centre for Climate Prediction and Research's freely available HadISST1 database ⁴⁶. The HadISST1 database provides global monthly SST on a 1° longitude × 1° latitude spatial grid and is available for all years since 1870. These data were used to examine temperature changes during the study period and to model the underlying processes of CTI.

Calculating community temperature index (CTI)

Community temperature index (CTI) is the abundance-weighted mean thermal affinity of a community or assemblage, which reflects the relative abundance of warm-affinity or cold-

affinity species⁵⁰. The inferred thermal affinity for each fish species in this study (1091 species total) was first calculated as the median temperature of each species' occurrences across its' global range of observations for which data were available (Figure S2). Rather than surface temperature or bottom temperature, we used mid-water-column temperature (i.e., from the surface to 200 meters depth) because the surveys included a mixture of demersal (bottomliving) and pelagic species. We used temperature climatologies from the global database WOD 2013 V2 (https://www.nodc.noaa.gov/cgi-bin/OC5/woa13/woa13.pl?parameter=t) with a spatial resolution of 1/4°. These climatologies represent average decadal temperatures for 1955-1964, 1965-1974, 1975-1984, 1985-1994, 1995-2004 and 2005-2012 on 40 depth layers. These data were aggregated vertically by calculating average temperature of the first 200 m depth. Species' occurrences were extracted from several databases including OBIS (https://obis.org/), **GBIF** (https://www.gbif.org/), VertNet (http://vertnet.org/) and ecoengine (https://ecoengine.berkeley.edu/). After removing duplicate occurrence records, we made a spatiotemporal match-up between temperature climatologies and species occurrences, considering both the geographic coordinates of occurrences, as well as their corresponding decade (to control for climate trends over the past 58 years). We then took the median value of temperature from these records for each species. Although we included both demersal and pelagic species and used mid-water-column temperature to infer thermal affinities in our analyses, we tested the sensitivity of our results to these choices by recalculating thermal affinities using surface temperature and bottom temperature, both with and without pelagic species (see Supplementary Material). Separate data sources were used to calculate species' thermal affinities and to model the underlying processes of CTI because estimating species' thermal affinities required matching species' occurrences with mid-water column temperatures, whereas modelling the underlying processes required a standardized, continuous, temporally resolved database. Mid-water-column data were only available as decadal averages and did not

384

385

386

387

388

389

390

391

392

393

394

395

396

397

398

399

400

401

402

403

404

405

406

407

408

cover the entire study period. Lastly, for each grid cell, we calculated the rate of change in SST and CTI as the slope of simple linear regressions of SST and CTI vs. time.

Comparison of thermal affinities with Cheung et al. 2013⁴

While a variety of past studies have quantified species' thermal affinities using species' distribution models⁵¹ or the midpoint of species minimum and maximum temperature observations²⁸, here we inferred thermal affinities as the median temperature value across a species' range of observations. To determine the accuracy of this approach, we compared our data with those of Cheung et al. 2013⁴ for 252 overlapping species. We found an 83% correlation between our data and those of Cheung et al. 2013⁴, indicating high consistency between the two studies. This provides strong support for our approach because Cheung et al. 2013⁴ is a landmark study investigating changes in the community temperature index in marine fishes.

QUANTIFICATION AND STATISTICAL ANALYSIS

All data handling and quantitative analyses were performed using R⁴⁵ version 4.0.0.

Decomposing CTI into the four underlying processes

CTI is a community weighted mean and therefore reflects changes in the relative abundances of warm-affinity and cold-affinity species. CTI will increase when species with thermal affinities greater than the mean of the community increase and when species with thermal affinities lower than the mean of the community decrease. Conversely, CTI will decrease when

species with thermal affinities greater than the mean of the community decrease and when species with thermal affinities lower than the mean of the community increase. Hence, CTI changes can be decomposed into four underlying process - tropicalization (increasing warmaffinity species), deborealization (decreasing cold-affinity species), borealization (increasing cold-affinity species), and detropicalization (decreasing warm-affinity species). The overall change in CTI reflects the relative strength of these processes. For instance, CTI will increase when the strength of tropicalization + deborealization is greater than the strength of borealization + detropicalization. To determine the strength of each underlying process, species within each grid cell must first be classified as either warm-affinity or cold-affinity. Because CTI (the mean thermal affinity of the community) changes every year, species may be warmaffinity one year (i.e., having a thermal affinity higher than the community mean) and coldaffinity the next (i.e., having a thermal affinity lower than the community mean). Therefore, to classify species as either warm or cold affinity within each grid cell, we used the mean CTI value across all years in the time series (i.e., mean of CTI values for 1990 to 2015 for each grid cell). We then separated warm and cold-affinity species into those that increased in abundance and those that decreased (Figure 1). Because CTI will shift up or down based on the amount of increase or decrease in species abundances along the thermal affinity axis (i.e., Figure 1), the strength of each process can be thought of as the amount of "pull" that each process exhibits on the overall community mean. This is determined by the degree to which species contributing to each process influence the overall community mean. Species that have thermal affinities much greater or much lower than the community mean will exhibit more influence than those with thermal affinities very similar to the mean. Additionally, species with large abundance changes will exhibit more influence than those with small abundance changes. Hence, each species contribution to the change in CTI is a combination of the difference between its individual thermal affinity (STI) and that of the community (CTI) and its change in abundance. We

431

432

433

434

435

436

437

438

439

440

441

442

443

444

445

446

447

448

449

450

451

452

453

454

455

therefore calculated the strength of each processes by (i) calculating the difference between each species' thermal affinity and the mean of the community, (ii) multiplying this value by each species' change in abundance, and (iii) taking the sum of the resulting values for all species within each process (Figure S3). We assessed the accuracy of this approach by comparing the value of (tropicalization + deborealization) – (borealization + detropicalization) to the rate of change in CTI for each grid cell. Note, these two values will never be a perfect match because, as mentioned above, some species fluctuate between warm and cold-affinity over time, especially in grid cells where CTI is highly variable across years. However, we found a correlation of 0.85 between the two values, indicating that our metric for estimating the strength of the underlying processes accurately captured changes in CTI (Figure S4).

Conditions associated with the underlying processes

To identify the biotic and abiotic conditions associated with each underlying process, we modelled the difference in the strength of tropicalization vs. deborealization (i.e., tropicalization minus deborealization) when CTI increased, and the difference in the strength of borealization vs. detropicalization (i.e., borealization minus detropicalization) when CTI decreased. We used linear mixed effects models with Gaussian likelihood distributions and included survey campaign as a random effect (i.e., varying intercept). Explanatory variables were the rate of change in SST, initial (i.e., baseline) SST, mean-annual SST variation, depth, distance to the nearest human population center, mean maximum body size, community thermal diversity (CTDIV), and community thermal range (CTR). Initial SST was defined as the mean-annual SST for each grid cell for the period 1980-1989, the ten years prior to the study period. Depth was recorded during each trawl survey, and we calculated mean depth per grid cell. Distance to the nearest human population center came from Yeager at al.⁴⁷, which is calculated as the

straight-line distance to the nearest provincial capital as defined by the ESRI World Cities data set. Body size data came from the open-access trait database of Beukhof et al. 48. CTDIV was defined as the variation in thermal affinities in the community and was calculated as the abundance-weighted standard deviation of species' thermal affinities⁹. CTR describes whether species in the community have narrow or wide thermal ranges and was calculated as the abundance-weighted mean of species' thermal ranges⁹. Thermal ranges were defined as the difference between the 90th and 10th percentiles of species thermal affinity observations. For CTDIV, CTR, and mean body size, we took the mean across the first 10 years of the study period for each grid cell to define baseline conditions in community structure that may have shaped community responses to warming. All metrics were calculated for the entire community sampled in each grid cell. Hence, identical predictors were used for both models, rather than sub-setting predictors to only species contributing to tropicalization and deborealization or to borealization and detropicalization.

Species contributing to opposite processes

To identify differences between species contributing to borealization vs. deborealization, and between species contributing to tropicalization vs. detropicalization, we used linear mixed effects models with binomial likelihood distributions and grid cell nested in survey campaign as random effects (i.e., varying intercepts). In grid cells where CTI increased, explanatory variables included maximum thermal limit, thermal range, maximum body size, and whether species are commercially fished. In grid cells where CTI decreased, the same explanatory variables were used except that minimum thermal limit was used in place of maximum thermal limit. Maximum and minimum thermal limits were defined as the 90th and 10th percentiles of species thermal affinity observations, respectively, and species thermal ranges were defined as

the difference between the 90th and 10th percentiles. Body size again came from Beukhof et al. 48. We defined whether a species was commercially fished according to categories of commercial importance available from FishBase⁴⁹. Species listed as 'highly commercial', 'commercial', or 'minor commercial', were considered commercially fished, and species listed as 'of no interest', 'of potential interest', 'subsistence fisheries', or 'unknown' were considered not commercially fished. All models were performed using the R package lme4⁵². Model quality and assumptions were verified using the R packages performance⁵³ and MuMin⁵⁴ (see Supplementary Material). Initial model inspection revealed low predictive accuracy and explained variation for the binomial models. This was likely because all species were initially included in this analysis whether they showed very slight or very large changes in abundance, i.e., any cold-affinity species whose change in abundance was greater than 0 was classified as contributing to borealization. All species populations fluctuate naturally, and so small increases or decreases in abundance are expected that may be independent of thermal affinity. Hence, including all species in this analysis could potentially blur patterns. We therefore reran models using i) all species, ii) species whose abundance changes were in the top 75%, iii) species whose abundance changes were in the top 50%, and iv) species whose abundance changes were in the top 25%. All approaches yielded very similar results, but with predictive accuracy and explained variation increasing with stricter species subsets. We therefore selected the model using species whose abundance changes were in the top 50% as a compromise between data deletion and model quality (at least 2000 observations per model and predictive accuracy over 70%), however, all model results are reported in Table S4.

525

526

504

505

506

507

508

509

510

511

512

513

514

515

516

517

518

519

520

521

522

523

524

Model performance

We assessed the performance of all models using the R package performance. For the two Gaussian models, we assessed linearity (i.e., residuals vs fitted values), homogeneity of variance, collinearity, the potential influence of high leverage observations, normality of residuals, and normality of random effects. This was accomplished with the function check_model. We also assessed predictive accuracy via the correlation between fitted values and observed values and via k-fold cross validation using the function performance_accuracy. Because cross validation results vary between iterations, we ran the performancy_accuracy function 99 times and recorded the average score. Both models satisfied all assumptions, including no high leverage observations and Variance Inflation Factors under 2.5 for all variables. For the model of differences between the strength of tropicalization and deborealization, the correlation between fitted values and observed values was 62% and the average cross validation accuracy was 57%. For the model of differences between the strength of borealization and deborealization, the correlation between fitted values and observed values was 79% and the average cross validation accuracy was 71%.

For the four binomial models, we assessed binned residuals and predictive accuracy using the functions binned_residuals and performance_accuracy. Binned residuals are assessed by first ordering predicted probabilities from smallest to largest and calculating raw residuals. Data are then split into bins of equal numbers of observations and the average residual is plotted against the average predicted probability for each bin. The quality of the model is then evaluated based on the percentage of binned residuals that lie within confidence limits/error bounds. Predictive accuracy was assessed as the area under the receiver operating characteristic curve (AUC – ROC), which evaluates how accurately a binomial model predicts group classification. AUC – ROC is bounded between 0 and 1, with 0 indicating 0% accuracy and 1 indicating 100% accuracy. For sites where CTI increased, the model of differences between species contributing to borealization and deborealization had 85% of residuals within error bounds and a predictive

accuracy of 73%, while the model of differences between species contributing to tropicalization and detropicalization had 84% of residuals within error bounds and a predictive accuracy of 73%. For sites where CTI decreased, the model of differences between species contributing to borealization and deborealization had 83% of residuals within error bounds and a predictive accuracy of 71%, while the model of differences between species contributing to tropicalization and detropicalization had 86% of residuals within error bounds and a predictive accuracy of 70%.

Altogether, these results show that our models did not violate assumptions, but that predictive accuracy was less than desirable. This likely indicates that other drivers that we were unable to assess are important in explaining variation in the strength of processes and in differences between species contributing to opposite processes. Further exploration showed that poor predictive accuracy may have also resulted from inconsistent relationships between surveys (i.e., regions). For example, including a random slope term for survey in the binomial models showed that, in sites where CTI decreased, upper thermal maximum was a strong predictor of whether species underwent borealization or derealization for all surveys except the Gulf of Alaska, Gulf of Mexico, and Baltic Sea. Additionally, commercially fished status was a strong predictor of whether species underwent borealization or deborealization in regions that were closer to human population centers, but not those that were further from population centers. However, models that included random slope terms did not have greater predictive accuracy, indicating that improving model accuracy ultimately hangs on uncovering other important drivers of process strength and species differences.

Sensitivity to pelagic species and temperature zone

To determine how including or excluding pelagic species influenced our results, we recalculated i) the rate of change in CTI, ii) the difference in the strength of tropicalization and deborealization, and ii) the difference in the strength of borealization and detropicalization after removing pelagic species. Additionally, to examine the impact of calculating thermal affinities with different water column zones (i.e., bottom temperature, mid-water-column temperature, and sea surface temperature) we recalculated the above three metrics using all three temperature zones. We did this for all possible scenarios, hence for all species using bottom, mid-water-column, and surface temperature, and for demersal species only using bottom, mid-water-column, and surface temperature. We then examined the correlation in metrics across all six scenarios. Across the six scenarios, correlation values for the rate of change in CTI ranged from 0.666 to 0.996 with a mean of 0.83, correlation values for the difference in the strength of tropicalization and deborealization ranged from 0.776 to 0.997 with a mean of 0.873, and correlation values for the difference in the strength of borealization and detropicalization ranged from 0.816 to 0.997 with a mean of 0.894, altogether indicating that results were robust to including or excluding pelagic species and to potential choices in thermal affinity calculation.

References

- 592 1. Chen, I.-C., Hill, J.K., Ohlemüller, R., Roy, D.B., and Thomas, C.D. (2011). Rapid Range 593 Shifts of Species Associated with High Levels of Climate Warming. Science *333*, 1024.
- 594 2. Pinsky, M.L., Worm, B., Fogarty, M.J., Sarmiento, J.L., and Levin, S.A. (2013). Marine taxa track local climate velocities. Science *341*, 1239–1242.
- Verges, A., Steinberg, P.D., Hay, M.E., Poore, A.G.B., Campbell, A.H., Ballesteros, E.,
 Heck, K.L., Booth, D.J., Coleman, M.A., Feary, D.A., et al. (2014). The tropicalization of
 temperate marine ecosystems: climate-mediated changes in herbivory and community
 phase shifts. Proc. R. Soc. B Biol. Sci. 281, 20140846–20140846.
- 600 4. Cheung, W.W., Watson, R., and Pauly, D. (2013). Signature of ocean warming in global fisheries catch. Nature *497*, 365–368.

- 5. Comte, L., Olden, J.D., Tedesco, P.A., Ruhi, A., and Giam, X. (2021). Climate and land-
- use changes interact to drive long-term reorganization of riverine fish communities
- 604 globally. Proc. Natl. Acad. Sci. 118, e2011639118.
- 605 6. Devictor, V., Van Swaay, C., Brereton, T., Chamberlain, D., Heliölä, J., Herrando, S.,
- Julliard, R., Kuussaari, M., Lindström, Å., and Roy, D.B. (2012). Differences in the
- climatic debts of birds and butterflies at a continental scale. Nat. Clim. Change 2, 121.
- 7. Cheung, W.W., Meeuwig, J.J., Feng, M., Harvey, E., Lam, V.W., Langlois, T., Slawinski,
- D., Sun, C., and Pauly, D. (2012). Climate-change induced tropicalisation of marine
- 610 communities in Western Australia. Mar. Freshw. Res. 63, 415–427.
- 8. Day, P.B., Stuart-Smith, R.D., Edgar, G.J., and Bates, A.E. (2018). Species' thermal
- ranges predict changes in reef fish community structure during 8 years of extreme
- temperature variation. Divers. Distrib. 24, 1036–1046.
- 9. Burrows, M.T., Bates, A.E., Costello, M.J., Edwards, M., Edgar, G.J., Fox, C.J., Halpern,
- 615 B.S., Hiddink, J.G., Pinsky, M.L., and Batt, R.D. (2019). Ocean community warming
- responses explained by thermal affinities and temperature gradients. Nat. Clim. Change 9,
- 617 959–963.
- 10. Vergés, A., Doropoulos, C., Malcolm, H.A., Skye, M., Garcia-Pizá, M., Marzinelli, E.M.,
- 619 Campbell, A.H., Ballesteros, E., Hoey, A.S., Vila-Concejo, A., et al. (2016). Long-term
- empirical evidence of ocean warming leading to tropicalization of fish communities,
- increased herbivory, and loss of kelp. Proc. Natl. Acad. Sci. 113, 13791–13796.
- 11. Bates, A.E., Pecl, G.T., Frusher, S., Hobday, A.J., Wernberg, T., Smale, D.A., Sunday,
- J.M., Hill, N.A., Dulvy, N.K., and Colwell, R.K. (2014). Defining and observing stages of
- climate-mediated range shifts in marine systems. Glob. Environ. Change 26, 27–38.
- 625 12. Horta e Costa B, Assis J, Franco G, Erzini K, Henriques M, Gonçalves EJ, and Caselle JE
- 626 (2014). Tropicalization of fish assemblages in temperate biogeographic transition zones.
- 627 Mar. Ecol. Prog. Ser. 504, 241–252.
- 628 13. Osland, M.J., Stevens, P.W., Lamont, M.M., Brusca, R.C., Hart, K.M., Waddle, J.H.,
- 629 Langtimm, C.A., Williams, C.M., Keim, B.D., and Terando, A.J. (2021). Tropicalization
- of temperate ecosystems in North America: The northward range expansion of tropical
- organisms in response to warming winter temperatures. Glob. Change Biol.
- 632 14. Pecuchet, L., Lindegren, M., Hidalgo, M., Delgado, M., Esteban, A., Fock, H.O., Gil de
- 633 Sola, L., Punzón, A., Sólmundsson, J., and Payne, M.R. (2017). From traits to life-history
- strategies: Deconstructing fish community composition across European seas. Glob. Ecol.
- 635 Biogeogr. 26, 812–822.
- 15. Beukhof, E., Frelat, R., Pecuchet, L., Maureaud, A., Dencker, T.S., Sólmundsson, J.,
- 637 Punzón, A., Primicerio, R., Hidalgo, M., Möllmann, C., et al. (2019). Marine fish traits
- follow fast-slow continuum across oceans. Sci. Rep. 9, 17878.
- 639 16. Duffy, J.E., Lefcheck, J.S., Stuart-Smith, R.D., Navarrete, S.A., and Edgar, G.J. (2016).
- Biodiversity enhances reef fish biomass and resistance to climate change. Proc. Natl.
- 641 Acad. Sci. 113, 6230–6235.

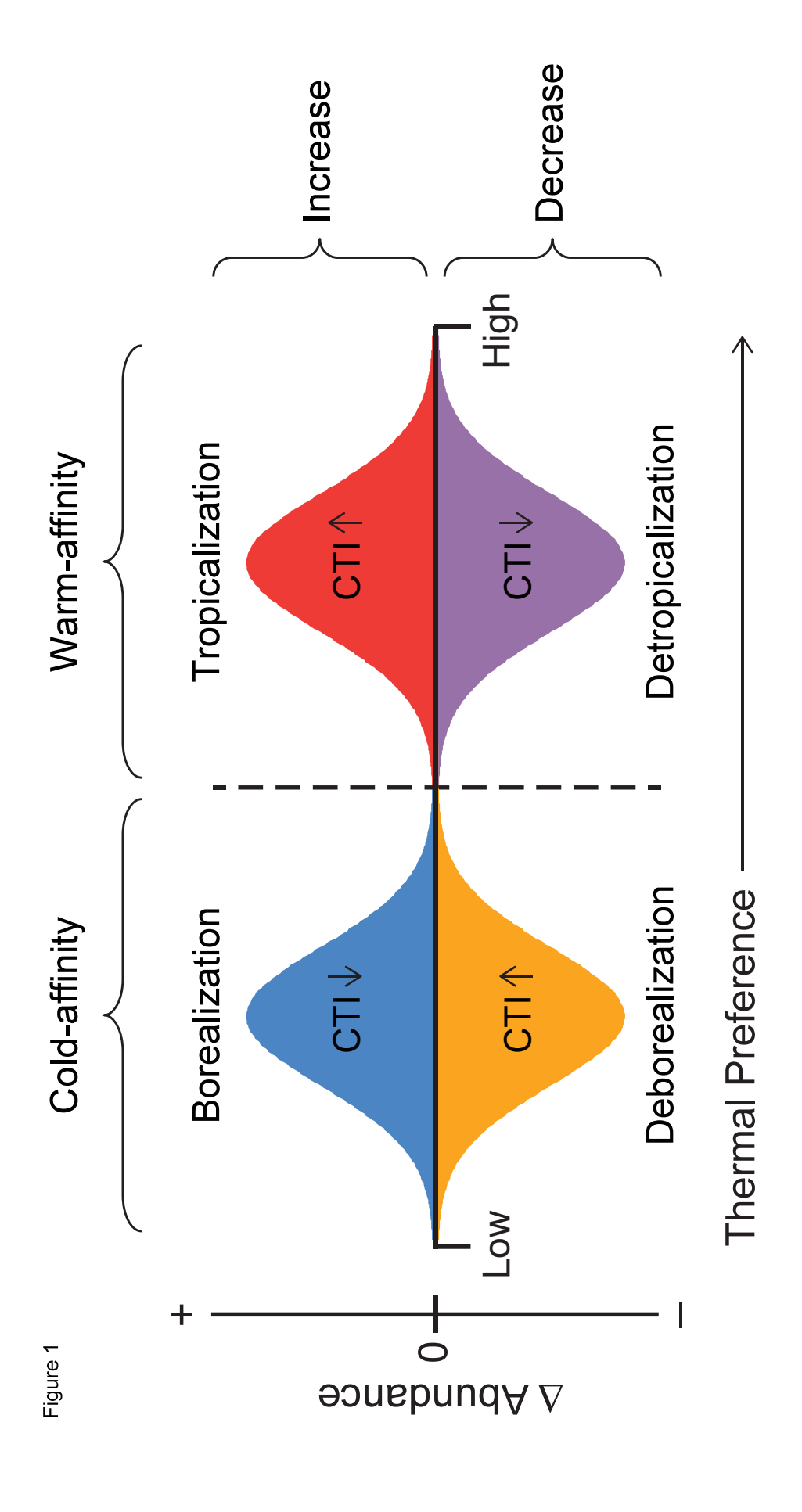
- 17. Maureaud, A., Hodapp, D., van Denderen, P.D., Hillebrand, H., Gislason, H., Spaanheden
- Dencker, T., Beukhof, E., and Lindegren, M. (2019). Biodiversity–ecosystem functioning
- relationships in fish communities: biomass is related to evenness and the environment, not
- to species richness. Proc. R. Soc. B Biol. Sci. 286, 20191189.
- 18. Maureaud, A., Andersen, K.H., Zhang, L., and Lindegren, M. (2020). Trait-based food
- web model reveals the underlying mechanisms of biodiversity–ecosystem functioning
- 648 relationships. J. Anim. Ecol. 89, 1497–1510.
- 649 19. Stuhldreher Gregor, Hermann Gabriel, and Fartmann Thomas (2014). Cold- adapted
- species in a warming world an explorative study on the impact of high winter
- temperatures on a continental butterfly. Entomol. Exp. Appl. 151, 270–279.
- 652 20. Pearce- Higgins James W., Eglington Sarah M., Martay Blaise, Chamberlain Dan E., and
- Both Christiaan (2015). Drivers of climate change impacts on bird communities. J. Anim.
- 654 Ecol. 84, 943–954.
- 21. Auber, A., Gohin, F., Goascoz, N., and Schlaich, I. (2017). Decline of cold-water fish
- species in the Bay of Somme (English Channel, France) in response to ocean warming.
- 657 Estuar. Coast. Shelf Sci. 189, 189–202.
- 22. Hiddink, J., and Ter Hofstede, R. (2008). Climate induced increases in species richness of
- marine fishes. Glob. Change Biol. 14, 453–460.
- 23. Barange, M., Merino, G., Blanchard, J.L., Scholtens, J., Harle, J., Allison, E.H., Allen,
- J.I., Holt, J., and Jennings, S. (2014). Impacts of climate change on marine ecosystem
- production in societies dependent on fisheries. Nat. Clim. Change 4, 211.
- 24. Antão, L.H., Bates, A.E., Blowes, S.A., Waldock, C., Supp, S.R., Magurran, A.E.,
- Dornelas, M., and Schipper, A.M. (2020). Temperature-related biodiversity change across
- temperate marine and terrestrial systems. Nat. Ecol. Evol. 4, 927–933.
- 666 25. Lenoir, J., Bertrand, R., Comte, L., Bourgeaud, L., Hattab, T., Murienne, J., and
- 667 Grenouillet, G. (2020). Species better track climate warming in the oceans than on land.
- 668 Nat. Ecol. Evol. 4, 1044–1059.
- 669 26. Fredston-Hermann, A., Selden, R., Pinsky, M., Gaines, S.D., and Halpern, B.S. (2020).
- 670 Cold range edges of marine fishes track climate change better than warm edges. Glob.
- 671 Change Biol. 26, 2908–2922.
- 672 27. Clarke, A., and Johnston, N.M. (1999). Scaling of metabolic rate with body mass and
- temperature in teleost fish. J. Anim. Ecol. 68, 893–905.
- 674 28. Stuart-Smith, R.D., Edgar, G.J., Barrett, N.S., Kininmonth, S.J., and Bates, A.E. (2015).
- Thermal biases and vulnerability to warming in the world's marine fauna. Nature 528,
- 676 88–92.
- 677 29. Jorda, G., Marbà, N., Bennett, S., Santana-Garcon, J., Agusti, S., and Duarte, C.M.
- 678 (2020). Ocean warming compresses the three-dimensional habitat of marine life. Nat.
- 679 Ecol. Evol. 4, 109–114.

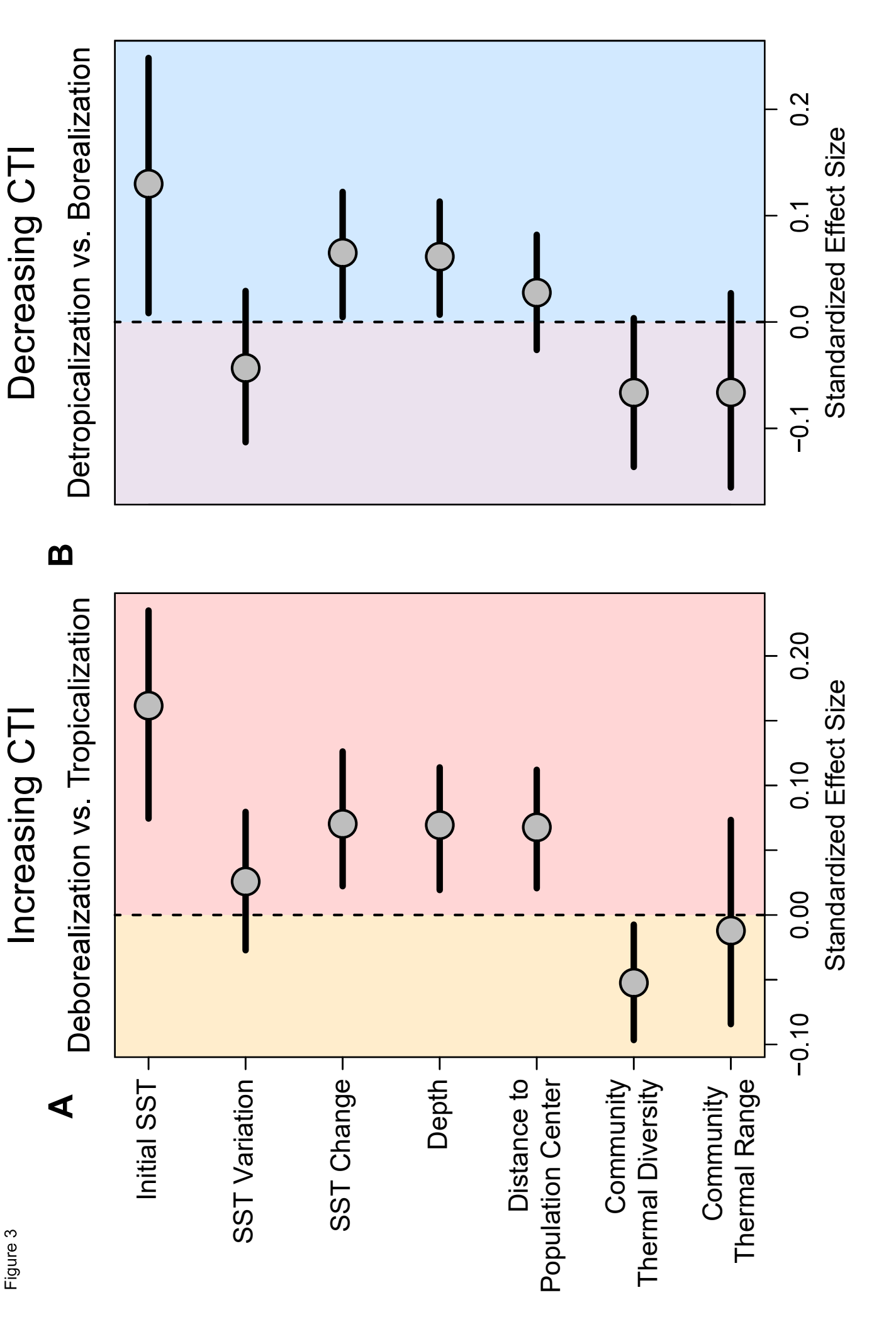
- 30. Dulvy, N.K., Rogers, S.I., Jennings, S., Stelzenmller, V., Dye, S.R., and Skjoldal, H.R.
- 681 (2008). Climate change and deepening of the North Sea fish assemblage: a biotic
- indicator of warming seas. J. Appl. Ecol. 45, 1029–1039.
- 31. Rutterford, L.A., Simpson, S.D., Jennings, S., Johnson, M.P., Blanchard, J.L., Schön, P.-
- J., Sims, D.W., Tinker, J., and Genner, M.J. (2015). Future fish distributions constrained
- by depth in warming seas. Nat. Clim. Change 5, 569.
- 686 32. Givan, O., Parravicini, V., Kulbicki, M., and Belmaker, J. (2017). Trait structure reveals
- the processes underlying fish establishment in the Mediterranean. Glob. Ecol. Biogeogr.
- 688 *26*, 142–153.
- 33. Beaugrand, G., Luczak, C., Goberville, E., and Kirby, R.R. (2018). Marine biodiversity
- and the chessboard of life. PLOS ONE 13, e0194006.
- 691 34. Bowler, D., and Böhning-Gaese, K. (2017). Improving the community-temperature index
- as a climate change indicator. PLOS ONE 12, e0184275.
- 693 35. McLean, M., Mouillot, D., Lindegren, M., Engelhard, G., Villéger, S., Marchal, P.,
- 694 Brind'Amour, A., and Auber, A. (2018). A climate-driven functional inversion of
- connected marine ecosystems. Curr. Biol. 28, 3654–3660.
- 696 36. McLean, M., Mouillot, D., and Auber, A. (2018). Ecological and life history traits explain
- a climate-induced shift in a temperate marine fish community. Mar. Ecol. Prog. Ser. 606,
- 698 175–186.
- 699 37. Mellin, C., Mouillot, D., Kulbicki, M., Mcclanahan, T.R., Vigliola, L., Bradshaw, C.,
- 700 Brainard, R., Chabanet, P., Edgar, G., and Fordham, D. (2016). Humans and seasonal
- climate variability threaten large-bodied coral reef fish with small ranges. Nat. Commun.
- 702 7, 1–9.
- 38. A Maureaud, A., Frelat, R., Pécuchet, L., Shackell, N., Mérigot, B., Pinsky, M.L.,
- Amador, K., Anderson, S.C., Arkhipkin, A., and Auber, A. (2021). Are we ready to track
- climate- driven shifts in marine species across international boundaries?- A global survey
- of scientific bottom trawl data. Glob. Change Biol. 27, 220–236.
- 39. Brander, K.M. (2007). Global fish production and climate change. Proc. Natl. Acad. Sci.
- 708 *104*, 19709–19714.
- 40. Wernberg, T., Bennett, S., Babcock, R.C., de Bettignies, T., Cure, K., Depczynski, M.,
- 710 Dufois, F., Fromont, J., Fulton, C.J., and Hovey, R.K. (2016). Climate-driven regime shift
- of a temperate marine ecosystem. Science 353, 169–172.
- 41. Gaines, S.D., Costello, C., Owashi, B., Mangin, T., Bone, J., Molinos, J.G., Burden, M.,
- Dennis, H., Halpern, B.S., and Kappel, C.V. (2018). Improved fisheries management
- could offset many negative effects of climate change. Sci. Adv. 4, eaao1378.
- 715 42. Goldenberg, S.U., Nagelkerken, I., Marangon, E., Bonnet, A., Ferreira, C.M., and
- Connell, S.D. (2018). Ecological complexity buffers the impacts of future climate on
- 717 marine consumers. Nat. Clim. Change 8, 229.

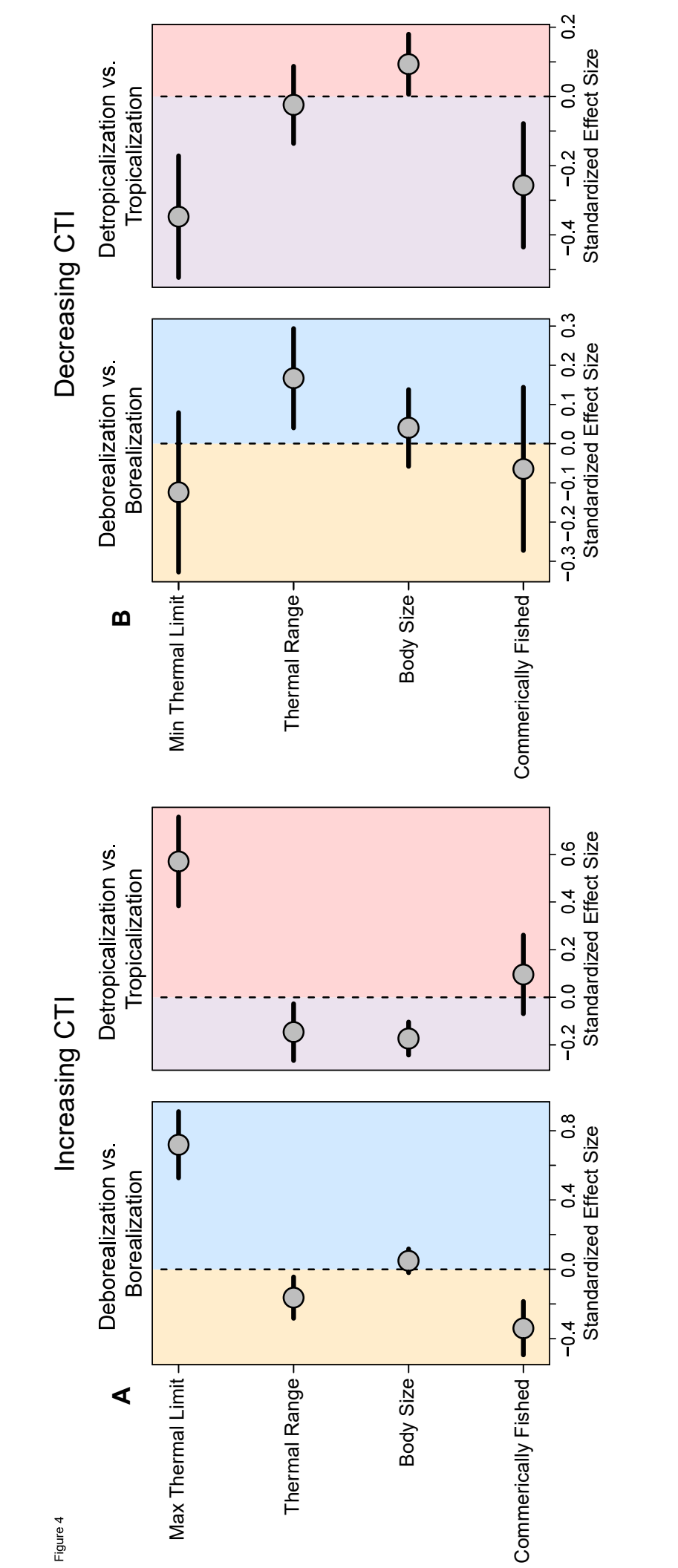
- 718 43. Cheung, W.W., Lam, V.W., Sarmiento, J.L., Kearney, K., Watson, R., Zeller, D., and
- Pauly, D. (2010). Large- scale redistribution of maximum fisheries catch potential in the
- global ocean under climate change. Glob. Change Biol. 16, 24–35.
- 44. Sumaila, U.R., Cheung, W.W., Lam, V.W., Pauly, D., and Herrick, S. (2011). Climate
- change impacts on the biophysics and economics of world fisheries. Nat. Clim. Change 1,
- 723 449–456.
- 45. Team, R.C. (2013). R: A language and environment for statistical computing.
- 46. Rayner, N., Parker, D., Folland, C., Horton, E., Alexander, L., and Rowell, D. (2003). The global sea-ice and sea surface temperature (HadISST) data sets. J Geophys Res *108*, 2–22.
- 727 47. Yeager, L.A., Marchand, P., Gill, D.A., Baum, J.K., and McPherson, J.M. (2017). Marine
- Socio-Environmental Covariates: queryable global layers of environmental and
- anthropogenic variables for marine ecosystem studies. Ecology 98, 1976–1976.
- 48. Beukhof, E., Dencker, T.S., Palomares, M.L.D., and Maureaud, A. (2019). A trait
- collection of marine fish species from North Atlantic and Northeast Pacific continental
- shelf seas. PANGEA.
- 733 49. Froese, R., and Pauly, D. (2010). FishBase (www database). Available at
- 734 http://www.Fishbase.org
- 735 50. Devictor, V., Julliard, R., Couvet, D., and Jiguet, F. (2008). Birds are tracking climate
- warming, but not fast enough. Proc. R. Soc. B Biol. Sci. 275, 2743.
- 51. Flanagan, P.H., Jensen, O.P., Morley, J.W., and Pinsky, M.L. (2019). Response of marine
- communities to local temperature changes. Ecography 42, 214–224.
- 739 52. Bates, D., Mächler, M., Bolker, B., and Walker, S. (2014). Fitting linear mixed-effects
- models using lme4. ArXiv Prepr. ArXiv14065823.
- 53. Lüdecke, D., Ben-Shachar, M.S., Patil, I., Waggoner, P., and Makowski, D. (2021).
- performance: An R package for assessment, comparison and testing of statistical models.
- J. Open Source Softw. 6.
- 744 54. Barton, K., and Barton, M.K. (2015). Package 'mumin.' Version 1, 439.

KEY RESOURCES TABLE

REAGENT		
or RESOURCE	SOURCE	IDENTIFIER
Software and	l algorithms	
Continui di di	The R	
R 4.0.0	Project for Statistical Computing ⁴⁵	https://cran.r-project.org/
Deposited Da	ata	
Fish monitoring data	OceanAdapt NOAA ²	https://oceanadapt.rutgers.edu/
Fish monitoring data	DATRAS ICES	https://datras.ices.dk/Data_products/Download/Download_Data_public.aspx
Fish monitoring data	IMR	https://www.hi.no/en/hi/forskning/research-data-1
Sea surface temperature data	Hadley Centre for Climate Prediction and Research ⁴⁶	https://www.metoffice.gov.uk/hadobs/hadisst/
Species occurrence data	OBIS	https://obis.org
Species occurrence data	GBIF	https://www.gbif.org
Species occurrence data	VertNet	http://vertnet.org
Species occurrence data	ecoengine	https://ecoengine.berkeley.edu
column	NOAA WOA 2013 V2 Database	https://www.nodc.noaa.gov/cgi-bin/OC5/woa13/woa13.pl?parameter=t
Distance to human population center data		https://esajournals.onlinelibrary.wiley.com/doi/full/10.1002/ecy.1884#support-information-section
Body size data	48	https://doi.pangaea.de/10.1594/PANGAEA.900866
Commercial fishing status data	FishBase ⁴⁹	http://www.fishbase.org







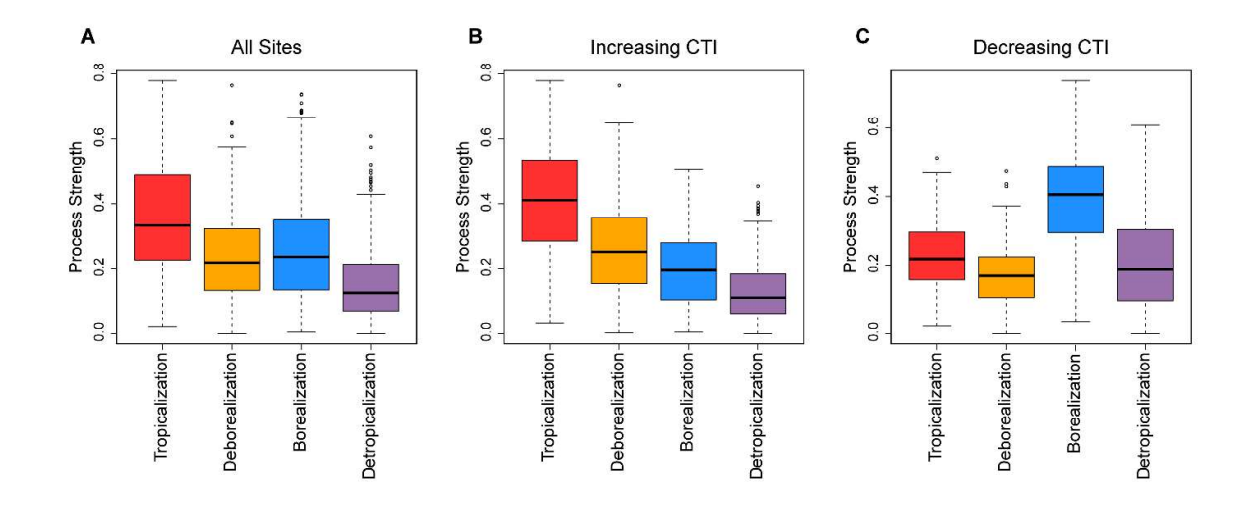


Figure S1. Boxplots of the strength of each of the underlying processes of CTI changes for all sites pooled (A), only sites where CTI increased over time (B), and only sites where CTI decreased over time (C), Related to Figure 2.

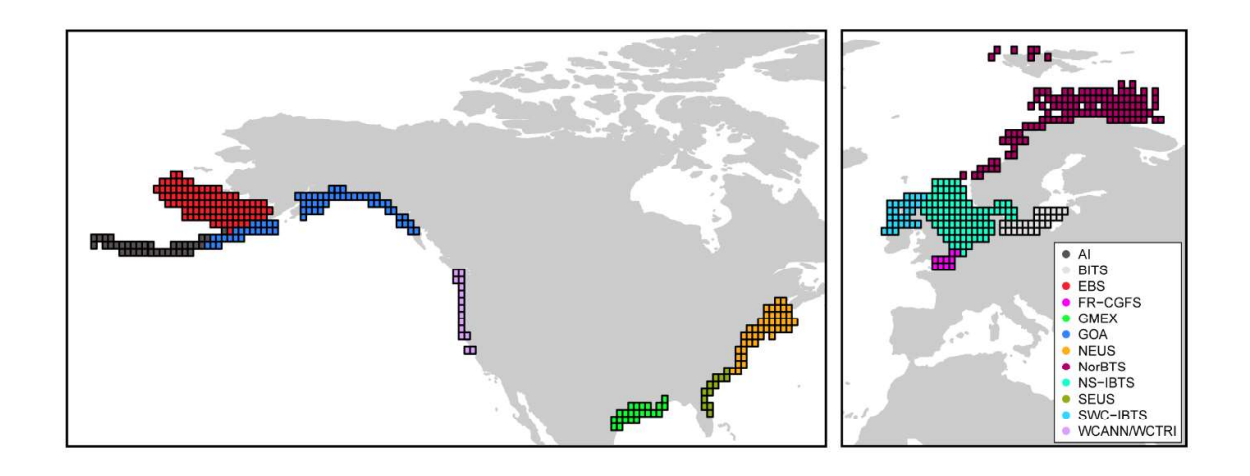


Figure S2. Map showing the spatial locations of the bottom trawl surveys used in the study, Related to Figure 2. Acronyms are defined in Table S1.

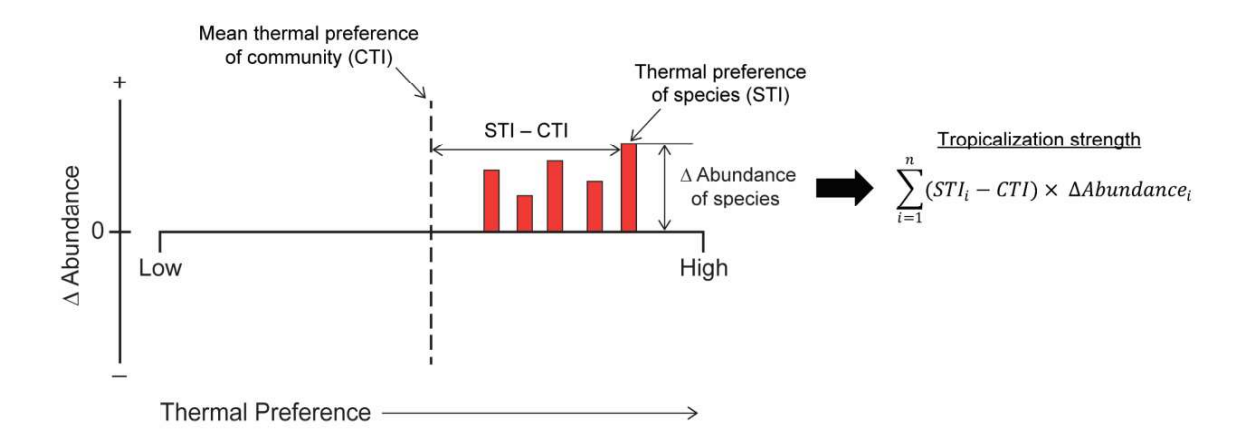


Figure S3. Method for calculating the strength of the underlying processes (tropicalization shown here), Related to Figure 2. First, the difference between each species individual thermal affinity (STI) and the mean thermal affinity of the community (mean CTI of all years for each site) is calculated (i.e., STI - CTI). Secondly, the resulting value is multiplied by species' individual changes in abundance (i.e., rate of change in abundance over time). Third, the sum of all resulting values is taken across all species.



CTI Rate of Change

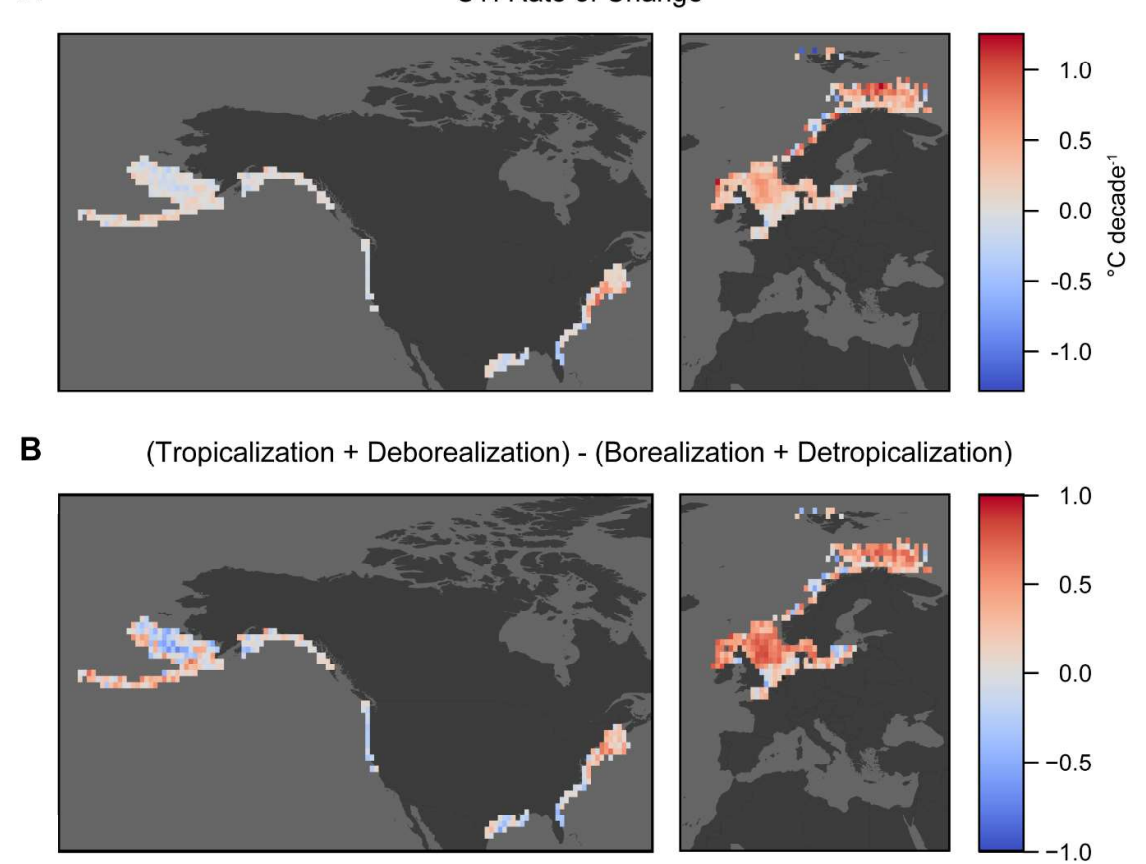


Figure S4. Maps of the rate of change in CTI (A) and the value of warm processes – cold processes, i.e., (topicalization + deborealization) – (borealization + detropicalization) (B), Related to Figure 2. The rate of change in CTI (A) and the value of warm processes – cold processes (B) had a correlation coefficient of 0.85.

Survey	Area	Years	Months	Source Reference
AI	Aleutian Islands	1991-2014	May – Sep	OceanAdapt NOAA ^{S1}
BITS	Baltic Sea 1991-2015 Jan. – Dec		DATRAS ICES ^{S2}	
EBS	BS East Bering Sea Shelf 1990-2015		May – Aug	OceanAdapt NOAA ^{S1}
FR-CGFS	East English Channel	1990-2015	Sep – Dec	DATRAS ICES ^{S2}
GMEX	Gulf of Mexico	1990-2015	May – Oct	OceanAdapt NOAA ^{S1}
GOA	Gulf of Alaska	1990-2015	May – Sep	OceanAdapt NOAA ^{S1}
NEUS	Northeast US	1990-2015	Feb – Dec	OceanAdapt NOAA ^{S1}
NorBTS	Norwegian Sea, Barents Sea	1990-2015	Jan – Dec	IMR ^{S3}
NS-IBTS	North Sea	1990-2015	Jan – Dec	DATRAS ICES ^{S2}
SEUS	Southeast US shelf	1990-2015	Apr – Nov	OceanAdapt NOAA ^{S1}
SWC-IBTS	Scotland Shelf Sea	1990-2015	Feb – Dec	DATRAS ICES ^{S2}
WCANN	West US Coast annual	2003-2015	May – Oct	OceanAdapt NOAA ^{S1}
WCTRI	West US Coast Tri-annual	1992-2004	May – Oct	OceanAdapt NOAA ^{S1}

 $Table \ S1. \ Metadata \ and \ sources \ for \ the \ thirteen \ bottom \ trawl \ survey \ campaigns \ used \ in \ this \ study, \ Related \ to \ Figure \ 2.$

	4.	on minus dal	h	han	minus datus		
	ti	op_minus_de	D	bor_minus_detrop			
Predictors	Estimates	CI	p	Estimates	CI	p	
Intercept	0.08	-0.06 - 0.22	0.271	0.14	-0.04 - 0.32	0.121	
SST Variation	0.03	-0.03 - 0.08	0.351	-0.04	-0.12 - 0.03	0.238	
SST Initial	0.16	0.09 - 0.23	<0.001	0.13	0.01 - 0.25	0.035	
SST Change	0.07	0.02 - 0.12	0.005	0.07	0.01 - 0.12	0.031	
Depth	0.07	0.02 - 0.12	0.003	0.06	0.01 - 0.11	0.024	
Distance to Market	0.07	0.02 - 0.11	0.004	0.03	-0.03 - 0.08	0.326	
CTDIV	-0.05	-0.100.01	0.022	-0.07	-0.14 - 0.01	0.069	
CTR	-0.01	-0.09 - 0.06	0.749	-0.07	-0.16 - 0.03	0.159	
Random Effects							
σ^2	0.05			0.03			
τ_{00}	0.05 _{surve}	ey		0.09 surve	ey		
ICC	0.51			0.72			
N	12 _{survey}			12 _{survey}			
Observations	398			160			
Marginal R ² / Conditional R ²	nal R^2 / Conditional $R^2 = 0.100 / 0.559$ $0.135 / 0.761$						

Table S2. Summary tables for models of differences in the strength of the underlying processes, Related to Figure 3.

	deb_vs_bor_warming			trop_vs_detrop_warming			deb_vs_bor_cooling			trop_vs_detrop_cooling		
Predictors	Log- Odds	CI	p	Log- Odds	CI	p	Log- Odds	CI	p	Log- Odds	CI	p
Intercept	0.02	-0.44 – 0.48	0.934	0.72	0.12 - 1.33	0.019	0.66	0.38 - 0.94	<0.001	0.29	0.05 - 0.52	0.016
Commerically Fished	-0.34	-0.49 – -0.19	<0.001	0.10	-0.07 – 0.26	0.256	-0.06	-0.27 – 0.14	0.543	-0.26	-0.44 – -0.08	0.005
Body Size	0.05	-0.02 - 0.12	0.164	-0.17	-0.24 – -0.10	<0.001	0.04	-0.06 – 0.14	0.422	0.09	0.01 - 0.18	0.035
Thermal Range	-0.16	-0.28 – -0.04	0.007	-0.15	-0.27 - -0.03	0.016	0.17	0.04 - 0.29	0.010	-0.02	-0.14 - 0.09	0.670
Max Thermal Limit	0.72	0.53 - 0.91	<0.001	0.57	0.38 - 0.76	<0.001						
Min Thermal Limit							-0.12	-0.33 – 0.08	0.231	-0.35	-0.52 – -0.17	<0.001
Random Effects												
σ^2	3.29			3.29			3.29			3.29		
τ_{00}	0.19 site	:survey		0.18 site	survey		0.27 site	e:survey		0.23 site	e:survey	
	0.58 _{sur}			1.05 survey			0.10 survey			0.03 _{survey}		
ICC	0.19			0.27			0.10	-		0.07		
N	398 site			398 site			160 site			160 site		
	12 surve	y		12 surve	y		12 _{surve}	y.		12 surve	ey .	
Observations	4583			4670			2181			2615		
Marginal R ² / Conditional R ²	0.084 / 0.258		0.063 / 0.317			0.011 / 0.109			0.038 / 0.107			

Table S3. Summary tables for models of differences between species contributing to opposite processes, Related to Figure 4.

Increasin	g CTI: Debo	realization v	s. Borealizati	on									
Species subset	Max Thermal limit	Thermal range	Body size	Fished	Marginal R ² /Conditional R ²	Binned residuals	Predictive accuracy	Observations					
All species	0.52 [0.40, 0.65]	-0.13 [- 0.21, - 0.05]	0.07 [0.02, 0.12]	-0.39 [- 0.50, - 0.29]	0.054/0.156	86%	66.5%	8691					
Top 75%	0.66 [0.51, 0.82]	-0.16 [- 0.26, - 0.07]	0.05 [-0.01, 0.10]	-0.33 [- 0.45, - 0.20]	0.076/0.215	84%	68.7%	6639					
Top 50%	0.72 [0.53, 0.91]	-0.16 [- 0.28, - 0.04]	0.05 [-0.02, 0.12]	-0.34 [- 0.49, - 0.19]	0.084/0.258	85%	72.6%	4583					
Top 25%	0.99 [0.69, 1.28]	-0.30 [- 0.49, - 0.11]	0.04 [-0.06, 0.14]	-0.48 [- 0.72, - 0.25]	0.114/0.406	75%	79.8%	2351					
Increasin	Increasing CTI: Detropicalization vs. Tropicalization												
Species subset	Max Thermal limit	Thermal range	Body size	Fished	Marginal R ² / Conditional R ²	Binned residuals	Predictive accuracy	Observations					
All species	0.21 [0.11, 0.32]	-0.07 [- 0.15, - 0.01]	-0.13 [- 0.17, -0.09	-0.08 [- 0.18, 0.01]	0.015/0.117	90%	65.6%	10406					
Top 75%	0.26 [0.13, 0.39]	-0.06 [- 0.15, 0.03]	-0.15 [- 0.20, -0.10]	-0.09 [- 0.21, 0.04]	0.021/0.186	85%	68.5%	7277					
Top 50%	0.57 [0.38, 0.76]	-0.15 [- 0.27, - 0.03]	-0.17 [- 0.24, -0.10]	0.09 [- 0.07, 0.26]	0.063/0.317	84%	72.6%	4670					
Top 25%	1.10 [0.76, 1.39]	-0.29 [- 0.50, - 0.09]	-0.09 [- 0.20, 0.01]	0.17 [- 0.10, 0.45]	0.118/0.565	72%	81.2%	2222					
Decreasii		orealization v	s. Borealizat	ion				_					
Species subset	Min Thermal limit	Thermal range	Body size	Fished	Marginal R ² / Conditional R ²	Binned residuals	Predictive accuracy	Observations					
All species	-0.11 [- 0.26, 0.04]	0.11 [0.02, 0.20]	0.06 [-0.01, 0.13]	-0.06 [- 0.21, 0.09]	0.007/0.073	83%	66.8%	3970					
Top 75%	-0.08 [- 0.26, 0.10]	0.15 [0.04, 0.25]	0.05 [-0.03, 0.13]	-0.01 [- 0.18, 0.16]	0.008/0.093	86%	68.6%	3188					
Top 50%	-0.12 [- 0.33, 0.08]	0.17 [0.04, 0.29]	0.04 [-0.06, 0.14]	-0.06 [- 0.27, 0.14]	0.011/0.109	83%	71.0%	2181					
Top 25%	-0.17 [- 0.43, 0.10]	0.22 [0.04, 0.40]	0.15 [0.01, 0.30]	-0.14 [- 0.44, 0.16]	0.025/0.141	79%	73.4%	1169					
25% Decreasin	0.43, 0.10] ng CTI: Detr	0.40]		0.44, 0.16]	0.025/0.141	79%	73.4%	1169					
25% Decreasin	0.43, 0.10]	0.40]	0.30]	0.44, 0.16] ization Fished	0.025/0.141 Marginal R ² / Conditional R ²	79% Binned residuals	73.4% Predictive accuracy	0bservations					
25% Decreasing Species	ng CTI: Detr Min Thermal	0.40] opicalization Thermal	vs. Tropical	0.44, 0.16] ization	Marginal R ² /	Binned	Predictive						
Decreasin Species subset	0.43, 0.10] ng CTI: Detr Min Thermal limit -0.23 [-	opicalization Thermal range -0.01 [-	0.30] vs. Tropical Body size 0.04 [-0.02,	0.44, 0.16] ization Fished -0.18 [- 0.30, - 0.06] -0.21 [- 0.35, - 0.07]	Marginal R ² / Conditional R ²	Binned residuals	Predictive accuracy	Observations					
25% Decreasin Species subset All species Top	0.43, 0.10] ng CTI: Detr Min Thermal limit -0.23 [- 0.35, -0.10] -0.22 [-	opicalization Thermal range -0.01 [-0.09, 0.06] 0.01 [-	0.30] vs. Tropicali Body size 0.04 [-0.02, 0.10] 0.04 [-0.03,	0.44, 0.16] ization Fished -0.18 [- 0.30, - 0.06] -0.21 [- 0.35, -	Marginal R ² /Conditional R ²	Binned residuals	Predictive accuracy 65.6%	Observations 5129					
Decreasin Species subset All species Top 75% Top	0.43, 0.10] ng CTI: Detr Min Thermal limit -0.23 [- 0.35, -0.10] -0.22 [- 0.38, -0.07] -0.35 [-	0.40] opicalization Thermal range -0.01 [- 0.09, 0.06] 0.01 [- 0.07, 0.10] -0.02 [-	0.30] vs. Tropicali Body size 0.04 [-0.02, 0.10] 0.04 [-0.03, 0.10] 0.09 [0.01,	0.44, 0.16] ization Fished -0.18 [- 0.30, - 0.06] -0.21 [- 0.35, - 0.07] -0.26 [- 0.44, -	Marginal R ² / Conditional R ² 0.017/0.066 0.18/0.075	Binned residuals 86%	Predictive accuracy 65.6% 67.1%	Observations 5129 3959					

Table S4. Model coefficients and explained variation for i) all species, ii) species whose abundance changes were in the top 75%, iii) species whose abundance changes were in the top 50%, and iv) species whose abundances changes were in the top 25%, Related to Figure 4. Values shown for predictor variables are standardized effect sizes and 95% confidence intervals.

Supplemental References

- S1. https://oceanadapt.rutgers.edu/S5.
- S2. https://datras.ices.dk/Data_products/Download/Download_Data_public.aspx
- S3. https://www.hi.no/en/hi/forskning/research-data-1